The role of PALLD-STAT3 interaction in megakaryocyte differentiation and thrombocytopenia treatment

Guoming Li,[1*] Haojie Jiang,[1*] Lingbin Wang,[1] Tingting Liang,[1] Chen Ding,[1] Mina Yang,[1] Yingzhi Shen,[1] Min Xin,[2] Lin Zhang,[1] Jing Dai,[2] Xueqing Sun,[1] Xuejiao Chen,[3] Junling Liu[1,4] and Yanyan Xu[1]

[1]Department of Biochemistry and Molecular Cell Biology, Key Laboratory of Cell Differentiation and Apoptosis of Chinese Ministry of Education, Shanghai Jiao Tong University School of Medicine, Shanghai; [2]Department of Laboratory Medicine, Ruijin Hospital, Shanghai Jiao Tong University School of Medicine, Shanghai; [3]School of Basic Medicine, Hubei University of Arts and Science, Xiangyang, Hubei Province and [4]Shanghai Synvida Biotechnology Co., Ltd., Shanghai, China

**GL and HJ contributed equally as first authors.*

Correspondence: X. Chen
ruipiaoc@163.com

J. Liu
liujl@shsmu.edu.cn

Y. Xu
xuyanyan901@163.com

Received: February 7, 2024.
Accepted: May 21, 2024.
Early view: May 30, 2024.

https://doi.org/10.3324/haematol.2024.285242

Supplemental Data

Supplemental Materials and Methods

Mice

The mice were generated by Shanghai Model Organisms Center, Inc. (Shanghai, China), with loxP sites flanking the PALLD exon12 on a C57BL/6 genetic background. They were crossed with *Platelet factor 4* (*Pf4*)-Cre mice (The Jackson Laboratory, 008535, C57BL/6) to produce megakaryocyte/platelet-specific PALLD-deficient mice (*pf4-Cre*$^{+}$ *PALLD*$^{f/f}$, *PALLD*$^{-/-}$).[1,2] All knockout mouse lines were maintained on the C57BL/6 background and genotyped by polymerase chain reaction (PCR). The PCR primers for genotyping the *PALLD-floxed* mice were 5'-AGGCAAGCACTCTACCGACTA-3' and 5'-TAAATGCCACAGACAGAAACTACC-3'. The PCR primers for genotyping the *Pf4-Cre* mice were 5'-GGATAGCGGCAATTACAGAACACC-3' and 5'-AGAACAGGACTCAGCCGTAGCAG-3'. Shanghai Jiao Tong University School of Medicine Animal Care and Use Committee approved the animal research.

Antibodies and reagents

Anti-PALLD polyclonal antibodies, anti-GAPDH polyclonal antibodies and anti-STAT3 polyclonal antibodies were purchased from Proteintech (Wuhan, Hubei, CN). PE-conjugated anti-CD41 monoclonal antibody and APC-streptavidin were purchased from BD Biosciences (San Jose, CA, USA). Anti-HA agarose and EZ-Link (tm) Sulfo-NHS-LC-Biotin were purchased from Pierce (Rockford, IL, USA). Anti-CD42c polyclonal antibodies were purchased from LifeSpan BioSciences, Inc. (Seattle, WA, USA). Anti-CD42b monoclonal antibody was purchased from Emfret Analytics (Würzburg, Germany). Apyrase, PGE1, anti-FLAG M2 affinity gel, anti-FLAG M2 monoclonal antibody, anti-α-Tubulin monoclonal antibody, fibrinogen from human plasma, Leptomycin B solution from *Streptomyces* sp. and Ivermectin were purchased from Sigma-Aldrich (St Louis, MO, USA). Anti-Phospho-STAT3 (Tyr705) monoclonal antibody, anti-HA monoclonal antibody and SimpleChIP® Enzymatic Chromatin IP Kit (Magnetic Beads) were purchased from Cell Signaling Technology (Danvers, MA, USA). Alexa fluor 488-conjugated anti-mouse IgG antibody, rhodamine (TRITC)-conjugated anti-goat IgG antibody, Alexa fluor 647-conjugated anti-rabbit IgG antibody and secondary HRP-conjugated antibodies were purchased from Jackson

ImmunoResearch Laboratories (West Grove, PA, USA). Propidium iodide was purchased from Invitrogen (San Francisco, CA, USA). MegaCult™-C Collagen and Medium with Lipids was purchased from STEMCELL Technologies (Vancouver, B.C., Canada). Mouse thrombopoietin Elisa kit, anti-Nuclear Pore Complex Proteins antibody and anti-Histone H3 antibody were purchased from Abcam (Cambridge, UK). Nuclear and Cytoplasmic Protein Extraction Kit was purchased from Beyotime Biotech. Inc. (Shanghai, CN). AchE Stain was purchased from Baso Diagnostics Inc. (Zhuhai, Guangdong, CN). Recombinant Mouse Interleukin-3 (IL-3), recombinant Mouse Interleukin-6 (IL-6) and recombinant Mouse Interleukin-11 (IL-11) were purchased from ProSpec (Rehovot, Israel). Recombinant Human Thrombopoietin (TPO) was purchased from 3SBIO, Inc. (Shengyang, Liaoning, CN). All peptides were synthesized by ChinaPeptides Co., Ltd. (Wuhan, Hubei, CN).

Transmission electron microscopy

Washed platelets were fixed in 4% glutaraldehyde at 4℃ for 2 h. After being washed and post-fixed with 2% osmium tetroxide, the platelet pellets were dehydrated. Thin sections were stained with 2% uranyl acetate and lead citrate, and examined under a CM-120 transmission electron microscope (FEI Company, OR, USA).

Next-generation RNA-Seq

Total RNA was extracted using the TRIzol (Invitrogen) and evaluated using the NanoDrop 2000 spectrophotometer (Thermo Scientific). RNA integrity was assessed using the Agilent 2100 Bioanalyzer (Agilent Technologies).

The libraries were constructed using VAHTS Universal V6 RNA-seq Library Prep Kit. Transcriptome sequencing was conducted by OE Biotech Co., Ltd. (Shanghai, China). Briefly, libraries were sequenced on an Illumina Novaseq 6000 platform, and 150 bp paired-end reads were generated. Clean reads were mapped to the reference genome using HISAT.[3] FPKM of each gene was calculated and the read counts of each gene were obtained by HTSeq-count.[4] PCA analysis was performed using R (v3.2.0) to evaluate the biological duplication of samples. Differential expression analysis was performed using the DESeq2. The Gene Ontology (GO) was annotated using the Gene Ontology Database (http://www.geneontology.org/). The processed RNA-Seq data and aligned

reads were deposited in GEO (BioProject: PRJNA1034807).

Liquid chromatography-mass spectrometry (LC-MS)

LC-MS was performed in megakaryocyte lysate Co-IP with anti-PALLD antibody. The mixture of peptides was separated using Zorbax 300SB-C18 peptide trap columns (Agilent Technologies) and tandem mass spectrometry (Thermo Finnigan Q Exactive). Gel digestion, mass spectrometry analysis, and database search were performed at the Core Facility of Basic Medical Sciences, Shanghai Jiao Tong University School of Medicine.

Plasmid construction

Primers were designed based on the PALLD sequence (NM_001166110.2) and STAT3 sequence (NM_001369512.1) from the NCBI website. The target genes were amplified from HEK293T cDNA and then ligated into the pcDNA3.1-Flag or pXJ40-HA vectors, resulting in the generation of Flag-PALLD, Ha-STAT3, and truncated PALLD and STAT3 plasmids.

Protein-protein docking

The crystal structure of PALLD (PDB ID: 2DM2) and STAT3 (PDB ID: 6TLC) were downloaded from the Protein Data Bank. AlphaFold2 predicted structures were referenced to complete the missing PALLD residues. Molecular Operating Environment (MOE) was used to perform protein-protein docking. After the completion of dynamic simulations, the final docking structures were analyzed by the PISA interface server and visualized by PyMOL.

Coimmunoprecipitation (Co-IP)

HEK293T cells were transfected with various plasmids for 48 hours. Total protein was collected using lysis buffer. Protein concentrations were determined by bicinchoninic acid (BCA) assay. Co-IP was performed using anti-Flag M2 Affinity Gel (Sigma) or anti-HA Agarose (Pierce) according to the manufacturer's instructions. All samples were washed with cold TBS, and the precipitated protein was eluted by boiling with loading buffer.

Chromatin Immunoprecipitation (Ch-IP)

Ch-IP assay was performed as described before.[5] Briefly, cells were crosslinked and lysed to release chromatin and fragmented DNA. Anti-PALLD antibody and ChIP-Grade Protein G Magnetic Beads (Cell Signaling Technology) were used to pull down the antibody-protein-DNA complex. After decrosslinking and purification, the enriched DNA was analyzed by PCR or qPCR.

Supplemental figures and figure legends

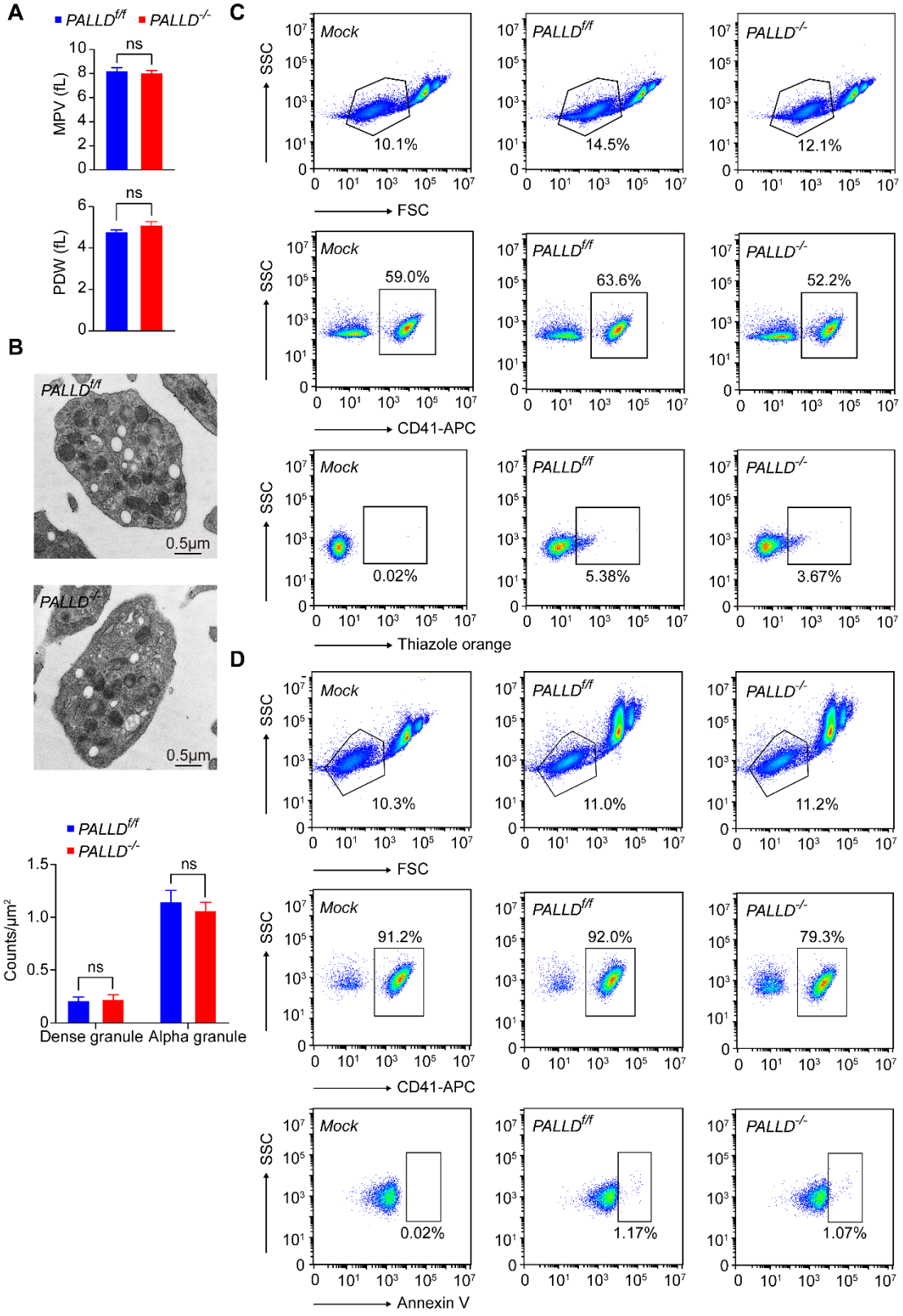

Supplemental Figure 1 (Figure S1)

(A) Mean platelet volume (MPV) and platelet distribution width (PDW) in *PALLD*$^{f/f}$ and *PALLD*$^{-/-}$ mice (n=7; ns, not significant).

(B) Representative images of *PALLD*$^{f/f}$ and *PALLD*$^{-/-}$ platelets under transmission electron microscopy. The scale bars represent 0.5 μm. Quantitative statistics of dense and alpha granules in *PALLD*$^{f/f}$ and *PALLD*$^{-/-}$ platelets (n=10; ns, not significant).

(C) Gating strategy for thiazole orange staining platelets in whole blood from *PALLD*$^{f/f}$ and *PALLD*$^{-/-}$ mice.

(D) Gating strategy for annexin V staining platelets in whole blood from *PALLD*$^{f/f}$ and *PALLD*$^{-/-}$ mice.

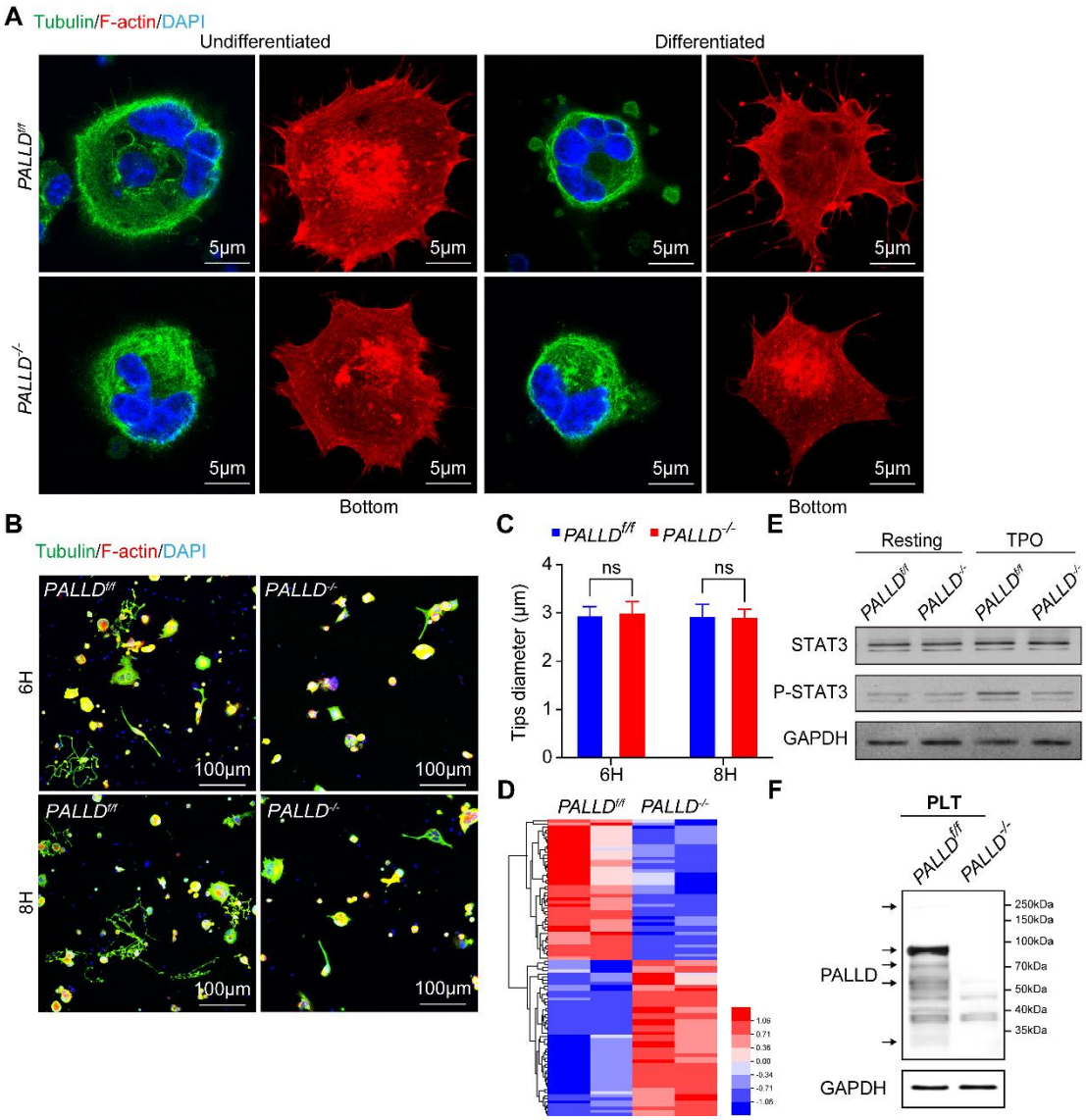

Supplemental Figure 2 (Figure S2)

(A) Immunofluorescence (IF) images of PPF-megakaryocytes derived from the fetal livers of *PALLD*$^{f/f}$ and *PALLD*$^{-/-}$ mice, stained for α-tubulin (Alexa Fluor 488) and F-actin (Rhodamine). The scale bars represent 5 μm.

(B) Representative low-magnification images of PPF-megakaryocytes derived from the fetal livers of *PALLD*$^{f/f}$ and *PALLD*$^{-/-}$ mice, stained for α-tubulin (Alexa Fluor 488) and F-actin (Rhodamine). The scale bars represent 100 μm.

(C) Proplatelet tip diameter in *PALLD*$^{f/f}$ and *PALLD*$^{-/-}$ megakaryocytes (6H, n=5; 8H, n=5).

(D) Heatmap for the clustering of differentially expressed genes in megakaryocytes.

(E) Western blot of the phosphorylation level of STAT3 Y705 in megakaryocytes treated with 25 IU/ml TPO.

(F) Western blot of PALLD expression in platelets of *PALLD*$^{f/f}$ and *PALLD*$^{-/-}$ mice.

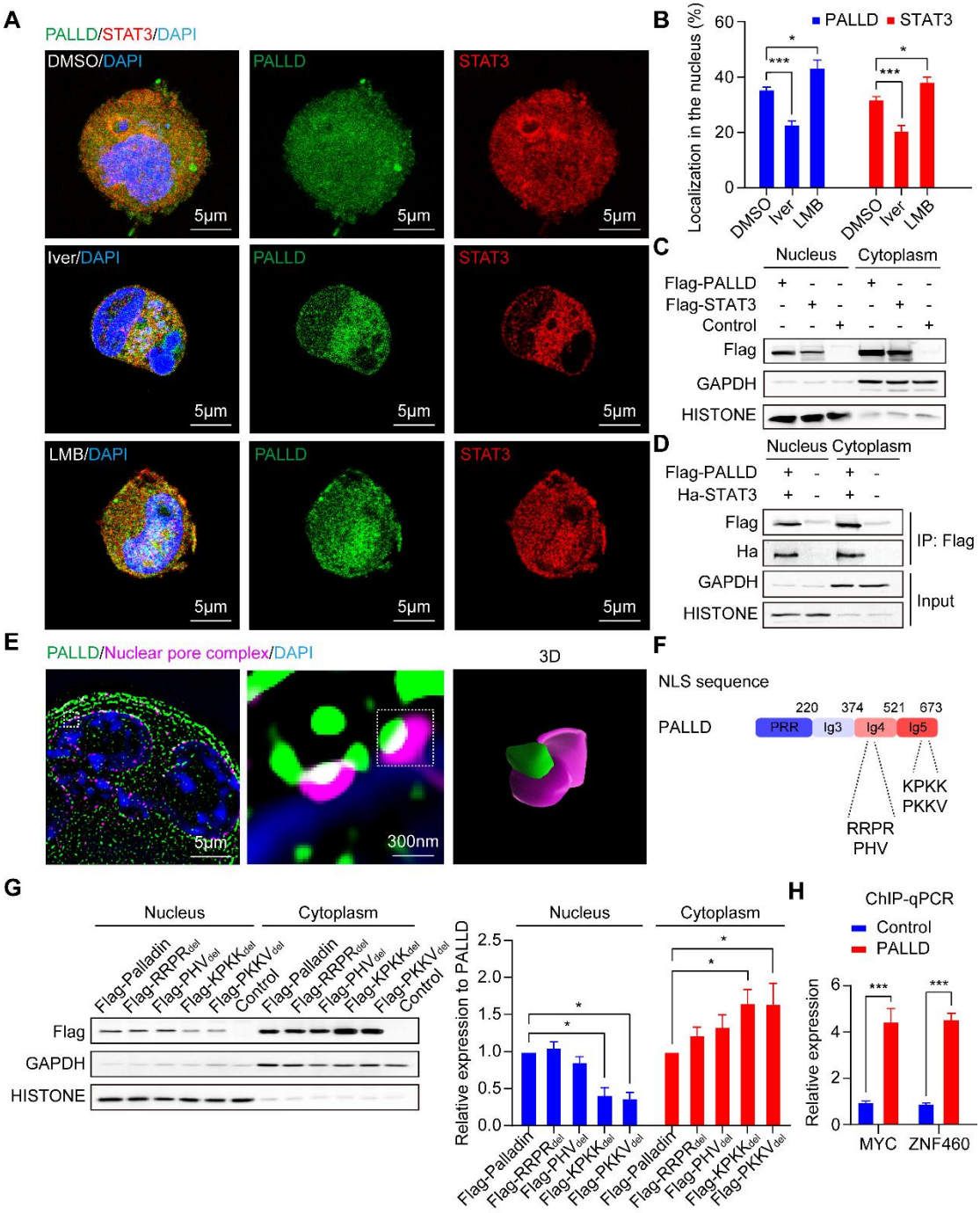

Supplemental Figure 3 (Figure S3)

(A-B) IF images of endogenous PALLD (Alexa Fluor 488) and STAT3 (Rhodamine) in fetal liver-derived megakaryocytes, treated with DMSO, Ivermectin (Iver), and Leptomycin B (LMB). Statistical analysis of PALLD and STAT3 localization is presented (n=5; *P<0.05, ***P<0.001). The scale bars represent 5 μm.

(C) Western blot results of Flag-PALLD or Flag-STAT3 expression in the nuclear and cytoplasmic fractions of transfected HEK293T cells.

(D) Co-IP of isolated nuclear and cytoplasmic proteins from HEK293T cells transfected with Flag-PALLD and Ha-STAT3.

(E) IF images of endogenous PALLD (Alexa Fluor 488) and nuclear pore complexes (Alexa Fluor 647) in megakaryocytes. 3D-volume rendering of PALLD and NPC signals using Imaris software. The scale bars represent 5 μm or 300 nm.

(F) Prediction of nuclear localization signals (NLSs) of PALLD performed by the PSORT.

(G) Western blot analysis of nuclear and cytoplasmic proteins from HEK293T cells transfected with Flag-PALLD lacking the predicted NLSs. Statistical analysis compared the expression levels of NLS-deleted PALLD with normal PALLD in the nucleus and cytoplasm. Statistical analysis of five independent experiments is shown (*$P<0.05$).

(H) QPCR analysis of chromatin immunoprecipitation (Ch-IP) samples from HEK293T cells transfected with Flag-PALLD, utilizing the STAT3-binding promoter sequence as primers. Statistical analysis of four independent experiments is shown (***$P<0.001$).

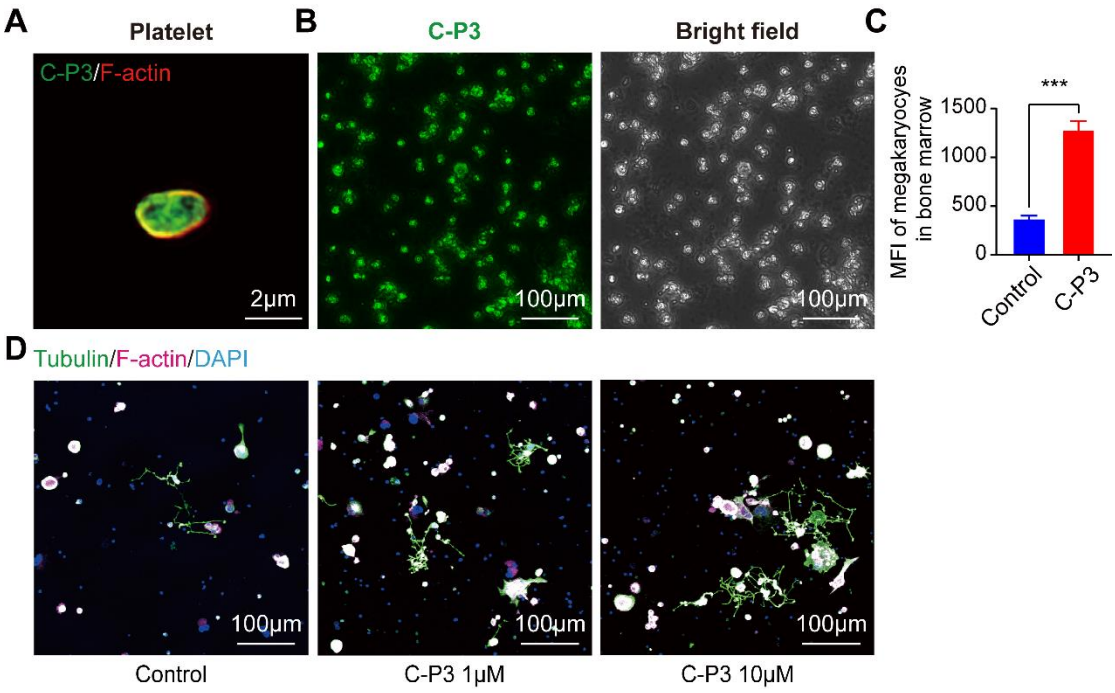

Supplemental Figure 4 (Figure S4)

(A) Representative IF images of platelets treated with FITC-labeled C-P3. The scale bars represent 2 μm.

(B) Representative images of bone marrow smear after bone marrow injection of FITC-labeled C-P3 in mice. The scale bars represent 100 μm.

(C) Mean fluorescence intensity (MFI) of megakaryocytes after bone marrow injection of FITC-labeled C-P3 or 0.9% NaCl in mice (n=4, ***P<0.001).

(D) Representative low-magnification images of fetal liver-derived megakaryocytes stimulated with PBS, or 1 μM and 10 μM C-P3. Stained for α-tubulin (Alexa Fluor 488) and F-actin (Alexa Fluor 647). The scale bars represent 100 μm.

Supplemental Table 1 (Table S1).

List of significantly regulated transcripts related to actin cytoskeleton dynamics.

Gene_id	Expression	FoldChange	P-value	Description
Wipf3	Down	0.218924509	0.017777	WAS/WASL interacting protein family, member 3
Ncald	Down	0.252921713	0.0162624	neurocalcin delta
Fscn1	Down	0.350748923	0.0188354	fascin actin-bundling protein 1
Coro2b	Down	0.38658607	0.0071098	coronin, actin binding protein, 2B

Supplemental Table 2 (Table S2).

List of significantly differentially expressed transcripts.

Gene_id	Expression	FoldChange	P-value	Description
4921536K21Rik	Down	0.029470413	0.0471659	RIKEN cDNA 4921536K21 gene
5430403G16Rik	Up	3.12113323	0.0135198	RIKEN cDNA 5430403G16 gene
6720489N17Rik	Up	2.119412345	0.005745	RIKEN cDNA 6720489N17 gene
AU041133	Up	3.557703218	0.015559	expressed sequence AU041133
AW146154	Up	2.018374121	0.0109815	expressed sequence AW146154
Acsbg1	Up	3.200249097	0.0024462	acyl-CoA synthetase bubblegum family member 1
Acsl6	Up	2.456645331	0.0091594	acyl-CoA synthetase long-chain family member 6
Adamdec1	Down	0.138071133	0.0131127	ADAM-like, decysin 1
Aldob	Up	4.290863573	0.0168796	aldolase B, fructose-bisphosphate
Alpk2	Down	0.24594861	0.0304378	alpha-kinase 2
Ano1	Up	56.37591771	0.009211	anoctamin 1, calcium activated chloride channel
Ano7	Down	0.015578367	0.0054534	anoctamin 7
Apol8	Up	2.261705442	0.0090452	apolipoprotein L 8
Asgr2	Down	0.202217223	0.0141571	asialoglycoprotein receptor 2
Atp9a	Down	0.379531755	0.006009	ATPase, class II, type 9A
B230307C23Rik	Up	2.139218799	0.0005539	RIKEN cDNA B230307C23 gene
B3galnt1	Down	0.459579376	0.0054401	Beta GlcNAc beta 1,3-galactosaminyltransferase, polypeptide 1
Bhlha15	Down	0.468517481	0.0009762	basic helix-loop-helix family, member a15
Bicd1	Up	2.001580012	0.0133114	BICD cargo adaptor 1
Cacna1h	Down	0.345234453	2.39E-09	calcium channel, voltage-dependent, T type, alpha 1H subunit
Cacna1s	Down	0.232007374	0.0001023	calcium channel, voltage-dependent, L type, alpha 1S subunit
Cadm3	Down	0.413712752	0.015913	cell adhesion molecule 3
Ccdc18	Up	2.27128765	0.0019961	coiled-coil domain containing 18
Cd300ld5	Down	0.0923159	0.0023615	CD300 molecule like family member D5
Cd59a	Up	2.031175596	0.0149283	CD59a antigen
Cep290	Up	3.242384053	8.60E-05	centrosomal protein 290
Cetn4	Up	3.138382804	0.0113273	centrin 4
Chst1	Down	0.201619597	1.21E-11	carbohydrate sulfotransferase 1
Cldn7	Down	0.112921016	0.0015498	claudin 7
Cntln	Up	2.016700549	4.13E-05	centlein, centrosomal protein
Coch	Up	18.16729941	0.0146526	cochlin

Col28a1	Up	2.020526789	0.0482233	collagen, type XXVIII, alpha 1
Colca2	Down	0.216483111	0.0003935	COLCA2 homolog
Coro2b	Down	0.38658607	0.0071098	coronin, actin binding protein, 2B
Cpeb3	Down	0.399083508	7.40E-05	cytoplasmic polyadenylation element binding protein 3
Csn3	Down	0.02825396	0.04444	casein kappa
Cxcl3	Up	4.215488079	0.008401	chemokine (C-X-C motif) ligand 3
Cxcl5	Up	3.446174755	0.0023923	chemokine (C-X-C motif) ligand 5
Cyp2b10	Down	0.090751224	0.0005473	cytochrome P450, family 2, subfamily b, polypeptide 10
D3Ertd751e	Up	2.376599844	7.75E-05	DNA segment, Chr 3, ERATO Doi 751, expressed
Derl3	Down	0.282094193	1.29E-07	Der1-like domain family, member 3
Dnm3	Down	0.186658931	0.0122665	dynamin 3
Efcab7	Up	2.384891377	0.0032613	EF-hand calcium binding domain 7
Ehf	Down	0.395467407	0.0117513	ets homologous factor
Epcam	Down	0.281942813	1.33E-06	epithelial cell adhesion molecule
Evc	Down	0.367751952	0.0114762	EvC ciliary complex subunit 1
F8	Up	3.585336831	0.0028301	coagulation factor VIII
Fam177a2	Up	5.76798945	0.002205	family with sequence similarity 177 member A2
Fam78b	Down	0.381849895	0.0496786	family with sequence similarity 78, member B
Fcrl5	Down	0.262818355	0.0012988	Fc receptor-like 5
Fosb	Up	2.17336952	1.32E-07	FBJ osteosarcoma oncogene B
Fosl1	Up	2.2636497	0.0107903	fos-like antigen 1
Fpr3	Down	0.169262714	2.11E-08	formyl peptide receptor 3
Fscn1	Down	0.350748923	0.0188354	fascin actin-bundling protein 1
Fut1	Down	0.30842056	0.0035429	fucosyltransferase 1
Gabra4	Down	0.274690113	0.0430881	gamma-aminobutyric acid (GABA) A receptor, subunit alpha 4
Gbgt1	Down	0.472155493	0.0376127	globoside alpha-1,3-N-acetylgalactosaminyltransferase 1
Gm14295	Up	2.239678618	0.0384968	predicted gene 14295
Gm1604b	Down	0.148767715	0.0029513	predicted gene 1604b
Gm2115	Down	0.015188976	0.0045465	predicted gene 2115
Gm3325	Up	2.454261648	4.29E-05	predicted gene 3325
Gm39469	Up	2.459609458	0.0058742	
Gm39701	Down	0.283576111	0.017259	
Gm45871	Up	2.050081653	0.0187758	predicted gene 45871
Gm46965	Up	2.513454774	0.0114312	
Gm4924	Up	3.89791226	0.0017019	
Gm5111	Up	4.497681186	0.0432071	predicted gene 5111
Gm51425	Up	2.235973714	0.0132717	predicted gene, 51425
Gm7072	Up	2.163085021	0.0005012	predicted gene 7072
Gpr55	Down	0.426431179	0.000151	G protein-coupled receptor 55
H2-M10.1	Down	0.139135025	0.0301976	histocompatibility 2, M region locus 10.1
Hba-a1	Up	2.115042324	1.91E-08	hemoglobin alpha, adult chain 1
Hba-a2	Up	2.224219996	5.43E-10	hemoglobin alpha, adult chain 2
Hbb-bs	Up	2.211920868	1.53E-07	hemoglobin, beta adult s chain
Hepacam2	Down	0.391319762	0.0001738	HEPACAM family member 2
Hmgn5	Up	2.701846976	2.54E-07	high-mobility group nucleosome binding domain 5
Hspa1b	Down	0.467078496	0.0421624	heat shock protein 1B

Ift74	Up	2.040261127	0.0063043	intraflagellar transport 74
Il12b	Down	0.022948436	0.0214607	interleukin 12b
Kcnt1	Up	37.59067702	0.0425164	potassium channel, subfamily T, member 1
Kif20b	Up	2.45576527	0.0267312	kinesin family member 20B
Krt222	Down	0.42695514	0.0212372	keratin 222
LOC101055663	Down	0.09467202	0.003845	
LOC118568705	Down	0.168884689	0.0431426	
Lilr4b	Up	2.113528037	8.36E-07	leukocyte immunoglobulin-like receptor, subfamily B, member 4B
Ly6a	Down	0.426466823	9.61E-06	lymphocyte antigen 6 complex, locus A
Ly6k	Down	0.318986321	0.0112939	lymphocyte antigen 6 complex, locus K
Mecom	Up	2.067623611	0.0487708	MDS1 and EVI1 complex locus
Mfsd4a	Down	0.348224939	0.0126334	major facilitator superfamily domain containing 4A
Msc	Down	0.021547467	0.0361376	musculin
Muc3a	Up	2.027574089	0.0023916	
Nanp	Down	0.227759362	0.0013142	N-acetylneuraminic acid phosphatase
Nbea	Down	0.308420126	0.0058014	neurobeachin
Ncald	Down	0.252921713	0.0162624	neurocalcin delta
Negr1	Down	0.100952369	2.41E-05	neuronal growth regulator 1
Nfkbiz	Up	2.017911653	1.78E-10	nuclear factor of kappa light polypeptide gene enhancer in B cells inhibitor, zeta
Nudt17	Up	3.975427795	0.0494299	nudix (nucleoside diphosphate linked moiety X)-type motif 17
Olfr414	Up	5.888517502	0.030644	olfactory receptor 414
Oosp1	Down	0.353386604	0.0002328	oocyte secreted protein 1
Osm	Up	2.006639369	4.59E-09	oncostatin M
Pgam2	Down	0.228030868	0.0019187	phosphoglycerate mutase 2
Pkhd1l1	Up	2.091841232	0.0021939	polycystic kidney and hepatic disease 1-like 1
Prlr	Down	0.365186526	0.045507	prolactin receptor
Ptn	Up	14.99225129	0.0220518	pleiotrophin
Rbp1	Up	2.092217038	0.0111178	retinol binding protein 1, cellular
Rd3l	Up	20.60192687	0.0397715	retinal degeneration 3-like
Rgs1	Up	2.370495828	4.42E-13	regulator of G-protein signaling 1
Robo1	Down	0.096858929	0.0197843	roundabout guidance receptor 1
Rwdd3	Up	2.668540682	0.0057974	RWD domain containing 3
Sapcd1	Up	2.261970036	0.0281879	suppressor APC domain containing 1
Sdc1	Down	0.385388762	4.58E-09	syndecan 1
Sfrp4	Up	3.22506314	0.0146541	secreted frizzled-related protein 4
Slc13a3	Down	0.47138114	0.0274589	solute carrier family 13 (sodium-dependent dicarboxylate transporter), member 3
Slc25a18	Up	4.983889324	0.0365861	solute carrier family 25 (mitochondrial carrier), member 18
Smim40	Down	0.217189057	0.049222	small integral membrane protein 40
Spag6	Down	0.113432273	0.0021743	sperm associated antigen 6
Spon1	Down	0.115395349	2.94E-16	spondin 1, (f-spondin) extracellular matrix protein
Tcf15	Up	3.538242341	0.043643	transcription factor 15
Tex11	Up	62.06689037	0.0060888	testis expressed gene 11
Tex15	Up	2.237253427	0.00031	testis expressed gene 15
Tex45	Up	3.625797023	0.0259027	testis expressed 45

Tnfrsf17	Down	0.209278987	4.38E-06	tumor necrosis factor receptor superfamily, member 17
Tuba3b	Down	0.029037126	0.0466667	tubulin, alpha 3B
Txndc5	Down	0.471851787	4.30E-07	thioredoxin domain containing 5
Wipf3	Down	0.218924509	0.017777	WAS/WASL interacting protein family, member 3
Zc3h6	Up	2.0176619	0.0002122	zinc finger CCCH type containing 6
Zfp40	Up	2.329059611	0.0017748	zinc finger protein 40
Zfp808	Up	2.1977959	0.0019538	zinc finger protein 808
Zfp820	Up	2.322840335	0.0405505	zinc finger protein 820
Zfp932	Up	2.086325592	4.88E-05	zinc finger protein 932
Zfp942	Up	2.002021322	0.0010809	zinc finger protein 942
Zfp948	Up	2.09951017	0.0046575	zinc finger protein 948
Zfp97	Up	2.178431962	0.0202292	zinc finger protein 97
Zfp970	Up	2.512347693	0.0072403	zinc finger protein 970
Zfp975	Up	2.677253478	0.0075524	zinc finger protein 975
Zfp976	Up	3.830148417	5.89E-05	zinc finger protein 976

Supplemental Table 3 (Table S3).

The information of each pathway in Figure 4C.

GO_id	Term	PopHits	-Log$_{10}$ (P value)	Enrichment_score
GO:0051491	Regulation of cell adhesion	20	2.209933603	16.87719298
GO:0042026	Protein refolding	24	2.054473874	14.06432749
GO:0007259	Receptor signaling pathway via JAK-STAT	32	1.813255551	10.54824561
GO:2001135	Regulation of endocytic recycling	34	1.763105141	9.927760578
GO:0080135	Regulation of cellular response to stress	6	1.74904339	4.018379282
GO:0003374	Dynamin family protein polymerization	35	1.739215251	9.644110276
GO:0032534	Regulation of microvillus assembly	42	1.590356599	8.036758563
GO:0006892	Post-Golgi vesicle-mediated transport	5	1.533432092	33.75438596
GO:0071803	Positive regulation of podosome assembly	48	1.482986373	7.032163743
GO:1903543	Positive regulation of exosomal secretion	7	1.389847724	24.11027569

Reference

1. Hitchcock IS, Kaushansky K. Thrombopoietin from beginning to end. British journal of haematology. Apr 2014;165(2):259-68. doi:10.1111/bjh.12772

2. Tiedt R, Schomber T, Hao-Shen H, Skoda RC. Pf4-Cre transgenic mice allow the generation of lineage-restricted gene knockouts for studying megakaryocyte and platelet function in vivo. Blood. Feb 15 2007;109(4):1503-6. doi:10.1182/blood-2006-04-020362

3. Kim D, Langmead B, Salzberg SL. HISAT: a fast spliced aligner with low memory requirements. Nature methods. Apr 2015;12(4):357-60. doi:10.1038/nmeth.3317

4. Anders S, Pyl PT, Huber W. HTSeq--a Python framework to work with high-throughput sequencing data. Bioinformatics (Oxford, England). Jan 15 2015;31(2):166-9.

doi:10.1093/bioinformatics/btu638

5. Mascanfroni ID, Yeste A, Vieira SM, et al. IL-27 acts on DCs to suppress the T cell response and autoimmunity by inducing expression of the immunoregulatory molecule CD39. Nature immunology. Oct 2013;14(10):1054-63. doi:10.1038/ni.2695